Nafertisite, $Na_3Fe^{2+}_{10}Ti_2(Si_6O_{17})_2O_2(OH)_6F(H_2O)_2$, from Mt. Kukisvumchorr, Khibiny alkaline massif, Kola peninsula, Russia: Refinement of the crystal structure and revision of the chemical formula

Fernando Cámara[1,2,3,*], Elena Sokolova[3], Yassir A. Abdu[3] and Frank C. Hawthorne[3]

[1] Dipartimento di Scienze della Terra, Università degli Studi di Torino, via Valperga Caluso 35, 10125 Torino, Italy
*Corresponding author, e-mail: fernando.camaraartigas@unito.it
[2] CrisDi - Interdepartmental Center for Crystallography, via Giuria 7, 10126 Torino, Italy
[3] Department of Geological Sciences, University of Manitoba, Winnipeg, Manitoba R3T 2N2, Canada

Abstract: The crystal structure of nafertisite, $Na_3Fe^{2+}_{10}Ti_2(Si_6O_{17})_2O_2(OH)_6F(H_2O)_2$, from Mt. Kukisvumchorr, Khibiny alkaline massif, Kola peninsula, Russia, a 5.358(1), b 16.204(3), c 21.976(4) Å, β 94.91(1)$^\circ$, V 1901.0(7) Å^3, space group $A2/m$, $Z = 2$, $D_{calc.}$ 3.116 g/cm^3, has been refined to an R_1 value of 5.60 % for 2747 observed $[F_o > 4\sigma F]$ unique reflections collected with a single-crystal diffractometer. The crystal used in the collection of the X-ray intensity data was analyzed by electron microprobe; the $Fe^{3+}/(Fe^{2+}+Fe^{3+})$ ratio was measured by Mössbauer spectroscopy, and FTIR and Raman spectra were collected. The empirical formula was calculated on the basis of $(O + F + OH + H_2O) = 44.39$ pfu: $(Na_{1.39}K_{0.61})_{\Sigma2}Na_1(Rb_{0.06}Cs_{0.02}\square_{0.92})_{\Sigma1}(Fe^{2+}_{9.11}Mg_{0.46}Mn_{0.22}Al_{0.10}Na_{0.09}Ca_{0.02})_{\Sigma10}(Ti_{1.90}Nb_{0.05}Mg_{0.03}Zr_{0.02})_{\Sigma2}[(Si_{11.81}Al_{0.19})_{\Sigma12}O_{34}]O_2(OH)_6(F_{0.86}O_{0.14})_{\Sigma1}(H_2O)_{1.39}$; $Z = 2$; the content of H_2O was calculated from the structure-refinement results. The HOH layer is the main structural unit in nafertisite. It consists of a central octahedral (O) sheet and two adjacent heteropolyhedral (H) sheets. The O sheet is composed of Fe^{2+}-dominant $M(1-3)$ octahedra, the $M(1-3)$ sites are fully occupied and the ideal composition of the O sheet is Fe^{2+}_{10} $apfu$. The H sheet is composed of the nafertisite T_6O_{17} ribbons and Ti-dominant D octahedra. The chemical composition of the nafertisite ribbon is $(Si_{11.81}Al_{0.19})O_{34}$ $apfu$, ideally $(Si_6O_{17})_2$ pfu. In the crystal structure of nafertisite, HOH layers alternate with intermediate (**I**) blocks along **c**. In the **I** block, the A, B, C and W sites are occupied by $(Na_{1.39}K_{0.61})$, Na, $(\square_{0.92}Rb_{0.06}Cs_{0.02})$ and $[(H_2O)_{1.39}\square_{0.61}]$ pfu, respectively. The chemical composition of the **I** block of the general formula A_2BCW is $[(Na_{1.39}K_{0.61})Na_1(\square_{0.92}Rb_{0.06}Cs_{0.02})(H_2O)_{1.39}]$ pfu, ideally $Na_3(H_2O)_2$ pfu. Nafertisite is closely related to the astrophyllite-group minerals.

Key-words: nafertisite; nafertisite T_6O_{17} ribbon; structure refinement; Mössbauer spectroscopy; FTIR spectroscopy; Raman spectroscopy; electron-microprobe analysis.

1. Introduction

A hypothetical *triple* ribbon of tetrahedra, $(Si_6O_{18})_n$, was first described by Layne *et al.* (1982). They also suggested coexistence of triple and double $(Si_4O_{12})_n$ astrophyllite ribbons in the astrophyllite structure. Khomyakov *et al.* (1995) and Ferraris *et al.* (1996) described nafertisite from Mt. Kukisvumchorr, Khibiny alkaline massif, Kola Peninsula, Russia, and reported its structure. Ferraris *et al.* (1996) studied nafertisite using scanning (SEM) and transmission (TEM) electron microscopy, X-ray powder diffraction and single-crystal X-ray diffraction. They solved the crystal structure of nafertisite in space group $A2/m$ to $R_1 = 0.26$ on a sample of fibrous nature with pervasive polytypic and polysomatic stacking disorder. Ferraris *et al.* (1996) introduced the HOH notation (O = octahedral sheet, H = heteropolyhedral sheet) for description of the HOH layer in the nafertisite structure and

reported the occurrence of a triple Si_6O_{17} ribbon in the H sheet. They classified the $[Si_{12}O_{34}]^{20-}$ anion as an *open branched zweier double chain* (in accord with Liebau, 1985). The topology of this ribbon is the same as the topology of the hypothetical *triple* ribbon of tetrahedra of Layne *et al.* (1982). Recently, the quadruple Si_8O_{22} ribbon of tetrahedra was discovered in the HOH structure of veblenite, $K_2\square_2Na(Fe^{2+}_5Fe^{3+}_4Mn_7\square)$ $Nb_3Ti(Si_2O_7)_2$ $(Si_8O_{22})_2O_6(OH)_{10}(H_2O)_3$ (Cámara *et al.*, 2013). By analogy with the double astrophyllite T_4O_{12} ribbon (Belov, 1976) and the quadruple veblenite T_8O_{22} ribbon (Cámara *et al.*, 2013), we suggest calling the ribbon described by Khomyakov *et al.* (1995) and Ferraris *et al.* (1996) the *nafertisite* T_6O_{17} ribbon. Khomyakov *et al.* (1995) and Ferraris *et al.* (1996) gave the simplified formulae of nafertisite ($Z = 2$): $Na_3(Fe^{2+},Fe^{3+})_6[Ti_2Si_{12}O_{34}](O,OH)_7$ $(H_2O)_2$ and $(Na,K)_3(Fe^{2+},Fe^{3+},\square)_{10}[Ti_2(Si,Fe^{3+},Al)_{12}$ $O_{37}](OH,O)_6$, respectively. Petersen *et al.* (1999) reported

a second occurrence of nafertisite from the Nanna Pegmatite, Narsaarsuup Qaava, South Greenland, and gave the following mineral formula: $Na_3Fe^{2+}_{10}Ti_2Si_{12}(O,OH,F)_{43}$, $Z = 2$. However, the results of the only structure work on nafertisite (Ferraris *et al.*, 1996) do not agree with its chemical analysis (Khomyakov *et al.*, 1995).

Here we resolve this problem and report the refinement of the crystal structure and a revised chemical formula of nafertisite from Mt. Kukisvumchorr, Khibiny alkaline massif, Kola Peninsula, Russia.

2. Previous work

Ferraris *et al.* (1996) considered the HOH layer as the main structural unit in the crystal structure of nafertisite. The central octahedral O sheet is composed of Fe-dominant M octahedra. Two adjacent H sheets are built of nafertisite T_6O_{17} ribbons and Ti-dominant D octahedra. Adjacent HOH layers link via X anions at common vertices of D octahedra, forming D-X-D bridges as in astrophyllite.

Here we outline some problems arising from the lack of agreement between structure-refinement results (Ferraris *et al.*, 1996) and chemical composition of nafertisite (Khomyakov *et al.*, 1995). The chemical analyses and empirical formulae for nafertisite from the Kola Peninsula, Russia [(1) this work; (2) Khomyakov *et al.* (1995)] and Greenland [(3) Petersen *et al.* (1999)] are given in Table 1. For samples (2) and (3), the sums of the cations are significantly different: 23.79 and 24.66 *apfu*,

respectively. Hence there is variation in chemical composition of nafertisite samples from different localities. As no structural data are available for sample (3), we will consider only the work of Khomyakov *et al.* (1995) and Ferraris *et al.* (1996), with empirical and simplified formulae of nafertisite given in Table 2. Table 3 gives unit-cell and structure-refinement parameters for nafertisite studied by Ferraris *et al.* (1996) and Table 4 gives atom coordinates and site occupancies for their structure model (labelling of atoms is taken from their work).

In the empirical formulae, Khomyakov *et al.* (1995) and Ferraris *et al.* (1996) assign $(Si_{10.36}Fe^{3+}_{1.64})_{\Sigma12}$ and $(Si_{10.36}Fe^{3+}_{1.24}Al_{0.40})_{\Sigma12}$ to the *Si* sites of two nafertisite ribbons (Table 2). Ferraris *et al.* (1996) reported on three Si(1–3) tetrahedra which constitute the nafertisite Si_6O_{17} ribbon, with $<Si(1–3)–O> = 1.62$, 1.62 and 1.64 Å. These Si–O distances are compatible with the ionic radius of [4]-coordinated Si = 0.26 Å, not of $^{[4]}Fe^{3+}$, with $r = 0.49$ Å (Shannon, 1976). Hence we conclude that there is no evidence of the presence of Fe^{3+} at the *Si* sites in the nafertisite ribbon.

Khomyakov *et al.* (1995) and Ferraris *et al.* (1996) give the composition of the O sheet as: $(Fe^{2+}_{4.68}Fe^{3+}_{1.27}Mg_{0.51}Mn_{0.18}\square_{3.36})_{\Sigma10}$ and $(Fe^{2+}_{4.68}Fe^{3+}_{1.67}Mg_{0.51}Mn_{0.18}\square_{2.96})_{\Sigma10}$, respectively (Table 2). Ferraris *et al.* (1996) reports three [6]-coordinated *Fe*(1,2,3) sites of the O sheet, with $<Fe(1–3)–\varphi> = 2.17$, 2.15 and 2.17 Å (φ = unspecified anion). The mean radii for cations at the *Fe*(1–3) sites, 0.79, 0.77 and 0.79 Å, are compatible with the ionic radius of [6]-coordinated

Table 1. Chemical composition and unit formula* of nafertisite from the Khibiny alkaline massif, Kola Peninsula, Russia [(1): this work; (2): taken from Khomyakov *et al.* (1995)] and the Igaliko nepheline syenite complex, Greenland [(3): taken from Petersen *et al.* (1999)].

Component (wt.%)	(1)	(2)	(3)	Formula unit (*apfu*)	(1)	(2)	(3)
Nb_2O_5	0.33	0.33	0.96	Nb	0.05	0.04	0.12
ZrO_2	0.11	n.d.	0.30	Zr	0.02	0	0.04
TiO_2	8.06	8.32	7.86	Ti	1.90	1.67	1.67
SiO_2	37.76	38.92	35.34	Si	11.81	10.36	9.96
Al_2O_3	1.08	1.32	3.69	Al	0.40	0.41	1.23
Fe_2O_3**		14.53		Fe^{3+}	0	2.91	0
FeO**	34.81	21.04	36.73	Fe^{2+}	9.11	4.68	8.67
MnO	0.82	0.79	1.94	Mn	0.22	0.18	0.46
CaO	0.06	n.d.	0.34	Ca	0.02	0	0.10
MgO	1.04	1.28	0.37	Mg	0.49	0.51	0.16
Cs_2O	0.12	n.d.	n.d.	Cs	0.02	0	0
Rb_2O	0.29	n.d.	n.d.	Rb	0.06	0	0
K_2O	1.52	1.64	2.09	K	0.61	0.56	0.75
Na_2O	4.09	4.78	2.74	Na	2.48	2.47	1.50
F	0.87	n.d.	0.86	Σcations	27.19	23.79	24.66
H_2O***	4.21	7.85	7.04				
O = F	–0.37		–0.36	F	0.86	0	0.77
Total	94.80	100.80	99.92	OH	6.0	2.0	13.23
				H_2O	1.39	5.97	0
				O^{2-}	36.14	35.02	29.00
				Σanions (*O* + F)	44.39	42.99	43.00

* calculated: on 44.39 (O + F + OH + H_2O) for (1), 43 O for (2) and 43 (O + F) where (OH + F) = 14 *apfu* for (3);
** Fe^{3+}/Fe^{2+} ratio determined from Mössbauer spectroscopy for (1) and (2);
*** determined from: structure refinement (1), wet chemistry (2) and stoichiometry (3);
n.d.: not detected.

Table 2. Empirical (EF), simplified (SF) and ideal (IF, ICF) formulae of nafertisite (previous work).

Interstitial cations	10 O-sheet cations	2D cations	$2(T_6O_{17})$ ribbons	Anions and H_2O groups
(1) Khomyakov *et al.* (1995)				
EF: $(Na_{2.47}K_{0.56})_{\Sigma3.03}$	$(Fe^{2+}_{4.68}Fe^{3+}_{1.27}Mg_{0.51}Mn_{0.18})_{\Sigma6.64}$	$(Ti_{1.67}Al_{0.41}Nb_{0.04})_{\Sigma2.12}$	$[(Si_{10.36}Fe^{3+}_{1.64})_{\Sigma12}O_{34}]$	$O_{1.02}(OH)_2 \cdot 5.97H_2O$
SF: Na_3	$(Fe^{2+},Fe^{3+})_6$	Ti_2	$[Si_{12}O_{34}]$	$(O,OH)_7 \cdot 2H_2O$
IF**: Na_2	$Fe^{2+}_5Fe^{3+}$	$[Ti_2$	$Si_{12}O_{34}]$	$O(OH)_6 \cdot 2H_2O$
(2) Ferraris *et al.* (1996)				
EF*: $(Na_{2.47}K_{0.56})_{\Sigma3.03}$	$(Fe^{2+}_{4.68}Fe^{3+}_{1.67}Mg_{0.51}Mn_{0.18})_{\Sigma7.04}$	$(Ti_{1.67}Nb_{0.04})_{\Sigma1.71}$	$[(Si_{10.36}Al_{0.40}Fe^{3+}_{1.24})_{\Sigma12}O_{34}]$	$O_{2.02}(OH)_2 \cdot 6.97H_2O$
SF: $(Na,K)_3$	$(Fe^{2+},Fe^{3+},\square)_{10}$	Ti_2	$[(Si,Fe^{3+},Al)_{12}O_{34}]$	$O_{3.0}(OH,O)_6$
ICF**: Na_3	$Fe^{2+}_9Fe^{3+}$	$[Ti_2$	$Si_{12}O_{34}]$	$O_3(OH)_6$

* quoted from Khomyakov *et al.* (1995);
** IF = ideal formula; ICF = ideal crystallochemical formula from the refined structural model, p. 6.

Table 3. Miscellaneous refinement data* for nafertisite.

	This work*	Ferraris *et al.* (1996)
a (Å)	5.358(1)	5.353(4)
b	16.204(3)	16.176(12)
c	21.976(4)	21.95(2)
β (°)	94.91(1)	94.6(2)
V (Å^3)	1901.0(7)	1894.41
Space group	$A2/m$	$A2/m$
Z	2	2
Absorption coefficient (mm^{-1})	4.56	
$F(000)$	1741.6	
$D_{calc.}$ (g/cm^3)	3.116	2.83
Crystal size (mm)	$0.200 \times 0.100 \times 0.010$	$0.72 \times 0.03 \times 0.02$
Radiation/filter	Mo$K\alpha$/graphite	Mo$K\alpha$/graphite
2θ-range for structure refinement (°)	60.21	40.0
R(int) (%)	4.48	
Reflections collected	47370	
Independent reflections	2900	491 ($F_o > 2\sigma F$)
$F_o > 4\sigma F$	2747	
Refinement method	Full-matrix least squares on F^2, fixed weights proportional to $1/\sigma F_o^2$	
No. of refined parameters	185	78
Final R(obs) (%)		
[$F_o > 4\sigma F$]	5.60	26.0 [$F_o > 2\sigma F$]
R_1	5.86	
wR_2	13.48	
Highest peak	1.57	
deepest hole (e Å^{-3})	-1.13	
Goodness of fit on F^2	1.271	

* refinement was done on the X-ray data collected from domain 1 (see text).

$Fe^{2+} = 0.78$ Å, not that for $^{[6]}Fe^{3+}$, $r = 0.645$ Å. We have found no evidence for the presence of Fe^{3+} in the nafertisite ribbon (see above) and in the O sheet of the HOH layer and therefore we conclude that $Fe^{3+}/Fe_{total} = 38$ % (Khomyakov *et al.*, 1995) is not correct.

Ferraris *et al.* (1996) reported the following site-occupancies for nafertisite: the three $Fe(1–3)$ sites are occupied by Fe at 80 % and ideally give $(Fe_8\square_2)$ *pfu.*; the *Ti* site ideally gives Ti_2 *apfu*; the *Na*(1) site gives 1 Na *apfu*; the *Na*(2) and *Na*(2)′ sites are 2.0 Å apart and can be only alternatively occupied, giving Na_2 *apfu*; in total, the *Na*(1,2,2′) sites give Na_3 *apfu*; the O(2) and O(5) atoms are OH groups, giving $(OH)_6$ *apfu*. Based upon the structure refinement of Ferraris *et al.* (1996) (Table 4) we write the ideal formula of nafertisite as follows $Na_3(Fe_8\square_2)Ti_2[(Si,Fe^{3+})_6O_{17}]_2O_3(OH)_6$, Z = 2 (Table 2). However, the latter formula does not agree with the ideal formulae of Khomyakov *et al.* (1995) and the ideal crystal-chemical formula of nafertisite based upon the structure model of Ferraris *et al.* (1996): $Na_2Fe^{2+}_5Fe^{3+}[Ti_2Si_{12}O_{34}]O(OH)_6(H_2O)_2$ and $Na_3Fe^{2+}_9Fe^{3+}[Ti_2Si_{12}O_{37}](OH)_6$, respectively (Table 2).

There is also disagreement in the numbers of H_2O and OH groups in the ideal crystal-chemical formula of nafertisite, $Na_3Fe^{2+}_9Fe^{3+}Ti_2 (Si_{12}O_{34})O_3(OH)_6$ [$H_2O = 0$ *pfu*, OH = 6 *pfu*], and its empirical formulae written by Khomyakov *et al.* (1995) [$H_2O = 5.97$ *pfu*; OH = 2 *pfu*] and Ferraris *et al.* (1996) [$H_2O = 6.97$ *pfu*; OH = 0 *pfu*] (Table 2). Presence of H_2O groups in the crystal structure of nafertisite was confirmed by the IR spectroscopy (Khomyakov *et al.*, 1995).

Based on the occupancies of three *Na* sites in the intermediate (**I**) block between the two HOH layers, the structure model gives the ideal composition of the **I** block as Na_3 *apfu*. However, only two of these three sites are coordinated by O atoms at reasonable Na–O distances; the third Na(2)′ site is lacking coordinating anions.

So with regard to nafertisite, we need to answer the following questions:

(1) What is the dominant cation species of the O sheet?
(2) What is the chemical composition of the nafertisite T_6O_{17} ribbon?
(3) What is the chemical composition of the intermediate (**I**) block?
(4) What is the chemical formula of nafertisite?

Table 4. Atom coordinates and equivalent* displacement parameters (Å^2) for nafertisite.

			This work				Ferraris *et al.* (1996)**					
Atom	W***	Site occ.(%)	x	y	z	U_{eq}	Atom	Site occ.(%)	x	y	z	U_{eq}
T(1)	8j	100	0.0403(2)	0.37743(8)	0.11463(6)	0.0094(3)	Si(1)	100	0.056(4)	0.378(1)	0.117(1)	0.073(8)
T(2)	8j	100	0.0434(2)	0.18783(8)	0.13156(6)	0.0100(3)	Si(2)	100	0.066(5)	0.188(2)	0.133(1)	0.042(9)
T(3)	8j	100	0.5444(2)	0.09413(8)	0.13617(6)	0.0111(3)	Si(3)	100	0.564(5)	0.092(1)	0.136(1)	0.030(8)
M(1)	8j	100	0.25692(12)	0.09978(4)	0.26372(3)	0.0118(2)	Fe(1)	80	0.258(2)	0.1006(8)	0.2649(6)	0.010(5)
M(2)	8j	100	0.24981(12)	0.29976(4)	0.24624(3)	0.0109(2)	Fe(2)	80	0.243(3)	0.3001(8)	0.2453(6)	0.016(5)
M(3)	4i	100	0.24396(17)	½	0.23267(5)	0.0119(3)	Fe(3)	80	0.242(3)	½	0.2319(9)	0.012(6)
D	4i	100	0.5346(2)	½	0.09789(5)	0.0092(3)	Ti	100	0.536(4)	½	0.0980(8)	0.005(6)
A(1)	4h	31	½	0.3121(8)	0	0.058(2)	Na(2)	?	½	0.346(4)	0	0.02(2)
A(2)	4h	59	½	0.3575(3)	0	0.0200(9)						
B	2a	100	0	½	0	0.0211(9)	Na(1)	100	0	½	0	0.05(2)
C	2b	8	0	0	0	0.14353(0)						
O(1)	8j	100	0.0666(6)	0.3927(2)	0.18833(16)	0.0135(7)	O(3)	100	0.089(8)	0.396(2)	0.186(2)	0.01(1)
O(2)	8j	100	0.2191(7)	0.0849(2)	0.41601(18)	0.0198(8)	O(9)	100	0.247(12)	0.082(4)	0.421(3)	0.06(2)
O(3)	8j	100	0.2772(7)	0.4152(3)	0.08399(17)	0.0200(8)	O(8)	100	0.275(9)	0.411(3)	0.081(2)	0.01(1)
O(4)	8j	100	0.0350(7)	0.2780(2)	0.10069(17)	0.0179(7)	O(10)	100	0.045(8)	0.278(3)	0.100(2)	0.01(1)
O(5)	8j	100	0.0706(6)	0.1943(2)	0.20539(15)	0.0117(6)	O(1)	100	0.113(8)	0.199(3)	0.206(2)	0.02(2)
O(6)	8j	100	0.2838(6)	0.1387(2)	0.10893(17)	0.0177(7)	O(11)	100	0.298(10)	0.140(4)	0.105(3)	0.05(2)
O(7)	8j	100	0.2158(6)	0.3597(2)	0.39084(18)	0.0188(8)	O(7)	100	0.215(8)	0.362(2)	0.391(2)	0.02(1)
O(8)	8j	100	0.5708(6)	0.0965(2)	0.21087(16)	0.0128(6)	O(4)	100	0.609(10)	0.096(3)	0.207(3)	0.04(2)
O(9)	4i	100	0.5375(10)	0	0.1108(3)	0.0172(10)	O(12)	100	0.573(13)	0	0.105(3)	0.03(2)
X_D^O	4i	100	0.4385(9)	0	0.3196(2)	0.0138(9)	O(6)	100	0.425(13)	0	0.328(3)	0.02(2)
$X_A^O(1)$	4i	100	0.0765(9)	0	0.2183(2)	0.0142(9)	O(2)	100	0.110(13)	0	0.223(3)	0.03(2)
$X_A^O(2)$	8j	100	0.4313(6)	0.2055(2)	0.30195(16)	0.0143(7)	O(5)	100	0.396(9)	0.205(3)	0.305(2)	0.02(2)
X_D^P	2c	100	½	½	0	0.0120(10)	O(13)	100	½	½	0	0.00(2)
W	4h	69	½	0.2211(8)	0	0.044(3)	Na(2)′	?	½	0.221(6)	0	0.02(3)
H(1)	4i	100	0.028(17)	0	0.1744(9)	0.01709						
H(2)	8j		0.391(12)	0.204(4)	0.3447(13)	0.01717						

* isotropic displacement parameters for A(1), C, H(1) and H(2) atoms (this work) and for all atoms (Ferraris *et al.*, 1996);
** atom coordinates of Ferraris *et al.* (1996) were transformed to correspond to the same independent part of the unit cell: $0 \leq x \leq 1.0$; $0 \leq y \leq 0.5$; $0 \leq z \leq 0.5$; $x = 0.752$ for O(11) was corrected to $x = 0.702$ (misprint); Na(2) + Na(2)′ = 2Na; $(OH)_6 = (OH)_2[O(2)] + (OH)_4[O(5)]$;
*** W = Wyckoff positions are analogous for both sets of atom coordinates.

3. Description of the sample

We studied a sample of nafertisite from Mt. Kukisvumchorr, Khibiny alkaline massif, Kola peninsula, Russia. This sample was purchased from a dealer. This is very difficult material on which to work. Although the initial ''crystals'' appear large, up to 40 μm thick and 10 mm long, they are coated with iron oxide that has to be removed before many measurements can be made. Underneath this coating, crystals are deformed (with undulose extinction) and twinned. The presence of similar coating on crystals was described for sveinbergeite, an astrophyllite-group mineral (Khomyakov *et al.*, 2011). Numerous crystals were examined before we found a suitable single crystal for the structure refinement; this crystal is a blade flat on (001), long on [100] and 0.200 × 0.100 × 0.010 mm in size.

4. Mössbauer spectroscopy

Mössbauer spectroscopy was done in transmission geometry at room temperature (R*T*) using a ^{57}Co point source. The spectrometer was calibrated with the R*T* spectrum of α-Fe. The nafertisite spectrum (Fig. 1) was collected on a few crystal fragments stuck to a thin-glass slide that was mounted on a Pb disk with ∼300
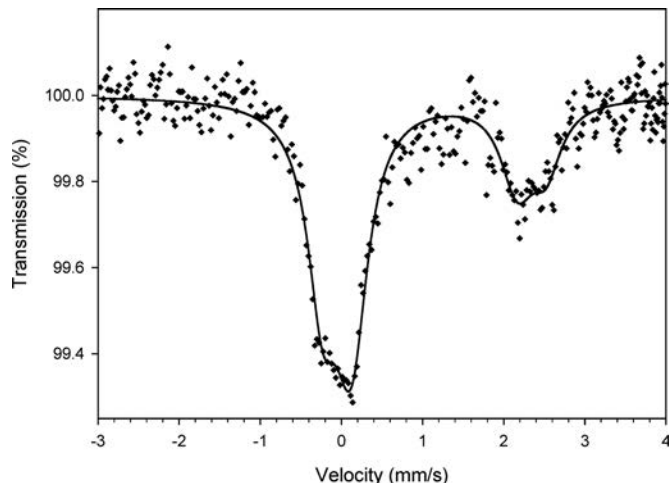
Fig. 1. The Mössbauer spectrum of nafertisite fitted with one QSD-site for Fe^{2+}.

μm aperture for a period of 4 months. It was fitted using a Voigt-based quadrupole-splitting-distribution (QSD) method to a model having only one QSD-site for Fe^{2+}, with two Gaussian components. The refined centre shift (CS), which is the same for the two components, is 1.14 mm/s, and the quadrupole splitting (Δ) parameters are $\Delta1 = 2.75$ mm/s and $\Delta2 = 2.05$ mm/s. The CS and Δ values are typical of Fe^{2+} in octahedral coordination. There is strong asymmetry in the spectrum which arises from preferred orientation of the two or three fibres that were used to collect the spectrum, and hence the ratio of the spectral areas of the low-velocity peak to the high-velocity peak was allowed to vary during spectrum fitting. This asymmetry and the statistical quality of the spectrum may mask a (very) small Fe^{3+} spectral contribution. However, when a significant amount of octahedrally coordinated Fe^{3+} is present, its high-velocity peak appears as a visible shoulder (at $\sim$0.7–1.0 mm/s) on the inner-side of the Fe^{2+} low-velocity peak, even in spectra with asymmetric doublets (*e.g.*, Abdu *et al.*, 2009; Sokolova *et al.*, 2013). Such a peak is not visible in the spectrum of nafertisite (Fig. 1) as it was, for example, in the spectrum of schüllerite (Sokolova *et al.*, 2013), and hence we can discount the presence of a significant amount of Fe^{3+} in nafertisite, in accord with the mean bond-lengths observed in the refined crystal-structure.

5. FTIR and Raman spectroscopy

Transmission FTIR spectra were obtained using a Hyperion 2000 IR microscope equipped with a liquid-nitrogen-cooled MCT detector. Spectra were collected on a thin film prepared by a Diamond Micro Compression Cell (Fig. 2a), and on the same single crystal used for collection of the X-ray diffraction data (Fig. 2b). Data over the range (4000–650 cm^{-1}) were obtained by averaging 100 scans with a resolution of 4 cm^{-1}. In the OH-stretching region (4000–3000 cm^{-1}), both thin-film and single-crystal FTIR spectra (Fig. 2a and b) show sharp peaks at 3653, 3626, 3604 and 3592 cm^{-1} that are attributable to OH-stretches of OH groups, and broad bands at $\sim$3400 and 3250 cm^{-1} (more visible in the single-crystal spectrum, Fig. 2b) due to stretching vibrations of H_2O, with H_2O bend peaks occurring at 1627 and 1640 cm^{-1} (shoulder). Strong bands at 1060, 983 (with a shoulder at $\sim$1010 cm^{-1}) and 923 cm^{-1}, along with a weak band at 679 cm^{-1} (Fig. 2a) may be assigned to Si-O stretches. The Si-O stretch region is not shown for the single-crystal spectrum (Fig. 2b) because of band saturation. Our FTIR results are in accord with those of Khomyakov *et al.* (1995), and indicate the presence of both OH and H_2O groups in the structure of nafertisite, with the former being the dominant species.

The Raman spectrum (100–1200 cm^{-1}, Fig. 2c), collected on the same nafertisite crystal used for the collection
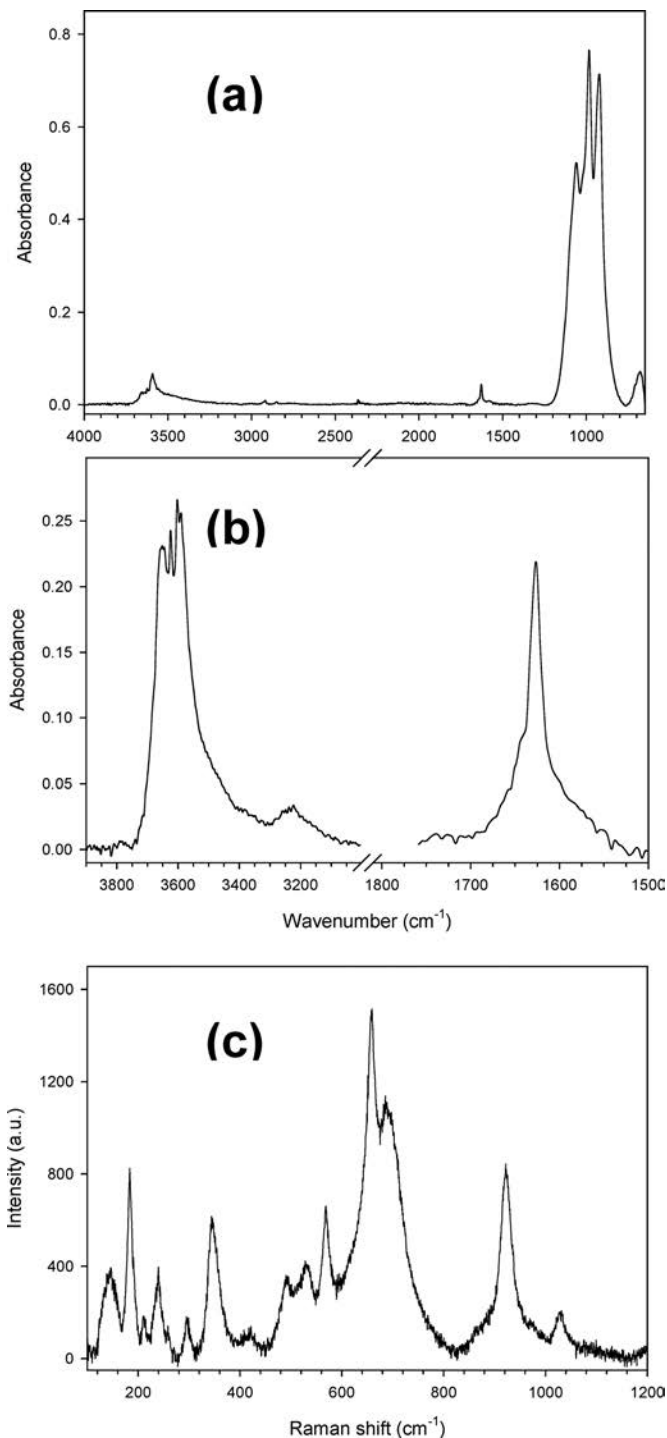
Fig. 2. FTIR, (a) thin film and (b) single crystal, and Raman (c) spectra of nafertisite.

of X-ray diffraction data, was acquired with a HORIBA Jobin Yvon-LabRAM ARAMIS integrated confocal micro-Raman system equipped with a 460 mm focal-length spectrograph and a multichannel air-cooled (-70°C) CCD detector. A magnification of 100x was used with an estimated spot size of $\sim$1 μm, a 1800 gr/mm grating, and a 633 nm excitation laser. The wavenumber

was calibrated using the 520.7 cm^{-1} line of Si metal. In the Raman spectrum of nafertisite (Fig. 2c), peaks at 1030, 922, 688 and 658 cm^{-1} may be assigned to Si-O stretches, and those at 569, 530, 490 and 420 cm^{-1} to bending modes of silicate groups. The peaks below ~400 cm^{-1} (345, 297, 240, 212, 184 and 145 cm^{-1}) are mainly due to lattice modes.

6. Electron-microprobe analysis

For the electron-microprobe analysis we used another crystal of nafertisite which was checked on the diffractometer and had dimensions $0.700 \times 0.100 \times 0.020$ mm. The crystal was placed on top of a resin disk, but not glued, and was coated with graphite. Because the crystal was very thin, the probe beam was possibly exciting not only the crystal but also the epoxy underneath the crystal, accounting for the low sum for the oxides (Table 1). The chemical composition of nafertisite was determined with a Cameca SX-100 electron-microprobe in wavelength-dispersion mode with an accelerating voltage of 15 kV, a specimen current of 10 nA, a beam size of 10 μm and count times on peak and background of 20 and 10 s, respectively. The following standards were used: titanite (Ti,Si), andalusite (Al), $Ba_2NaNb_5O_{15}$ (Nb), pollucite (Cs), Rb-leucite (Rb), zircon (Zr), diopside (Ca), fayalite (Fe), spessartine (Mn), forsterite (Mg), orthoclase (K), albite (Na) and F-bearing riebeckite (F). Ta, Zr, Cr, Sn, Ba, Sr, Pb, V and Zn were sought but not detected. Data were reduced using the PAP procedure of Pouchou & Pichoir (1985). The amount of H_2O was calculated from the structure refinement (see discussion below). The empirical formula was calculated on the basis of $(O + F + OH + H_2O) = 44.39$ *pfu*, the valence state of iron was determined by Mössbauer spectroscopy, the H_2O content was calculated from structure-refinement results and the presence of H_2O and OH groups was confirmed by FTIR spectroscopy: $(Na_{1.39}K_{0.61})_{\Sigma2}Na_1(\square_{0.92}Rb_{0.06}Cs_{0.02})_{\Sigma1}(Fe^{2+}_{9.11}Mg_{0.46} Mn_{0.22} Al_{0.10}Na_{0.09} Ca_{0.02})_{\Sigma10}(Ti_{1.90}Nb_{0.05}Mg_{0.03}Zr_{0.02})_{\Sigma2} [(Si_{11.81}Al_{0.19})_{\Sigma12}O_{34}]O_2(OH)_6(F_{0.86}O_{0.14})_{\Sigma1}(H_2O)_{1.39}$; $Z = 2$ [Table 1, analysis (1) and unit formula (1)].

Analyses (1) and (2) (Table 1) are very similar, as expected for nafertisite from the same locality. The principal difference is in the sum of the oxides: 94.80 wt.% for analysis (1) and 100.80 wt.% for analysis (2). One major difference between these two analyses is the value given for H_2O: 4.21 wt.% in analysis (1) *versus* 7.85 wt.% in analysis (2). Analysis (1) counted the H_2O groups in the refined crystal structure; analysis (2) was a bulk chemical analysis for H_2O. The latter is 85 % higher than the former, and such an amount of H_2O would show prominently in the crystal structure; it is not seen in our structure (see below), and we must conclude that this higher value is not correct. Using the H_2O value from analysis (1), the sum for analysis (2) should be reduced by $7.85–4.21 = 3.64$ wt.%. The Mössbauer results (see above) show that there is negligible

Fe^{3+} in nafertisite, and the analytical sum of analysis (2) should be reduced by $14.53–14.53/1.11134 = 1.46$ wt.%. The aggregate reduction in the sum for analysis (2) is $1.46 + 3.64 = 5.10$ wt.%, resulting in an analytical sum of $100.80–5.10 = 95.70$ wt.%. For analysis (1), because of the unconventional preparation of the crystal necessitated by its extremely acicular nature, the analytical sum is low due to either (i) the electron beam exceeding the bounds of the crystal or (ii) sample charging, or both. In analysis (3), the content of H_2O was calculated assuming $OH + F = 14$ anions per formula unit. This assumption is completely incompatible with the structure, which cannot accommodate that large number of OH groups (see Table 7).

7. The crystal structure

7.1. X-ray data collection and structure refinement

All crystals of nafertisite that we were able to find were twinned. The X-ray diffraction data for the twinned crystal of nafertisite were collected with a Bruker D8 three-circle diffractometer equipped with a rotating-anode generator, multilayer optics and an APEX-II detector (Mo$K\alpha$ radiation). The crystal consists of two domains related by 2-fold rotation (180°) around [100]. The volumes of the domains are related by the ratio 0.885(2) [domain 1]:0.115(2) [domain 2]. The intensities of 68238 reflections with $0 < h < 7, –22 < k < 0, –30 < l < 30$ were collected from both domains to 60.21° 2θ using 0.3° frame and an integration time of 12 s. The unit-cell parameters were obtained using CELL-NOW (Sheldrick, 2004) which provided two orientation matrices for the two domains. The unit-cell parameters (Table 3) were refined using 7553 reflections from both components with $I > 10\sigma I$ (4054 reflections from the first domain) and an empirical absorption correction (TWINABS, Sheldrick, 2008a) was applied. The proportion of reflections rejected due to overlap was 27 %. The crystal structure of nafertisite was refined using X-ray single-crystal data from the first domain to an R_1 value of 5.60 %, with the Bruker SHELXTL Version 5.1 system of programs (Sheldrick, 2008b) (Table 3); initial atom coordinates were taken from Ferraris *et al.* (1996). Scattering curves for neutral atoms were taken from International Tables for Crystallography (Wilson, 1992). Site-scattering values were refined for the $M(1–3)$ sites with the scattering curve of Fe, D site (scattering curve of Ti), $A(1)$ site (scattering curve of K), $A(2)$ and B sites (scattering curve of Na), C site (scattering curve of Cs) and W site (O). For the B site, refinement converged to an integer value and hence it was subsequently fixed at full occupancy. For nafertisite, we observed disorder at the $A(1)$, $A(2)$ and W sites, partly occupied by K, Na and H_2O and separated by short distances: $A(1)–A(2) = 0.74$ and $A(1)–W = 1.47$ Å. At the last stages of the refinement, two peaks were found in the difference-Fourier map (with residual electron density of 1.44 and 0.96 e$^-$/Å^3) which were included in the refinement as the H(1) and H(2) atoms. The D(donor)-H

distances were softly constrained to 0.98 Å. For the final refinement, the occupancies for $A(1,2)$, C and W sites were adjusted in accord with chemical analysis and fixed, with the occupancies for the $A(2)$ and W sites being equal (see text below). Details of the data collection and structure refinement are given in Table 3, final atom parameters are given in Table 4, selected interatomic distances in Table 5, refined site-scattering values and assigned populations for selected cation sites are given in Table 6, and bond-valence values in Table 7. Anisotropic displacement parameters, a table of structure-factors and a CIF file are available online as supplementary material linked to this article on the GSW website of the journal, http://eurjmin.geoscienceworld. org.

7.2. Site-population assignment

In accord with the nomenclature for the astrophyllite-group minerals (Sokolova, 2012), we divide the cation sites into three groups: M sites of the O sheet, D and T sites of the H sheet, and interstitial A, B and C sites in the intermediate (**I**) block.

Consider first the Ti-dominant $^{[6]}D$ site in the H sheet. The refined site-scattering value at the D site is 44.6 $epfu$ and we assign 1.90 Ti + 0.05 Nb + 0.02 Zr + 0.03 Mg, with the calculated site-scattering 45.01 $epfu$. There are three T sites, with $<< T\text{–}O>> = 1.627$ Å (Table 5), a typical Si–O distance in accord with the absence of Fe^{3+} in

the nafertisite ribbon. To the three T sites, we assign all available Si (Table 1) and add Al to achieve 12 $apfu$: $(Si_{11.81}Al_{0.19})_{\Sigma12}$ (Table 6).

Consider next the interstitial sites in the **I** block. The A site splits into $A(1)$ and $A(2)$ sites, separated by a short distance of 0.74 Å (Table 5) and hence can be alternatively occupied by cations, with A(1) + A(2) = 2 $apfu$. Such split of the A site into two sites occupied mainly by K (rarely Cs) and Na (rarely Li) is characteristic of several astrophyllite-group minerals (Cámara $et\ al.$, 2010). In nafertisite, the refined site-scattering at the [9]-coordinated $A(1)$ site is 11.59 $epfu$, $<A(1)\text{–}\varphi> = 3.157$ Å (Table 5) and we assign all 0.61 K $apfu$ (Table 1) to this site: [1.39 $\square$ + 0.61 K] pfu (Table 6). At the [6]-coordinated $A(2)$ site, the refined site-scattering is 15.59 $epfu$, $<A(2)\text{–}\varphi> = 2.397$ Å and we assign 1.39 Na $apfu$ to the $A(2)$ site: [1.39 Na + 0.61 $\square$] pfu (Table 6). At the $A(2)$ site, Na is coordinated by five O atoms and an H_2O group at the W site (Tables 5 and 6). There is a short distance $W\text{–}A(1) = 1.42$ Å and hence the W and $A(1)$ sites can be only alternately occupied. The $A(1)$ site is occupied by K at 30 % (see above), and therefore the W site can be occupied by H_2O at 70 %, $i.e.$, by 1.39 H_2O pfu which is in accord with 1.39 Na $apfu$ at the $A(2)$ site (Table 6). We assign Na to the [10]-coordinated B site [as for the majority of the astrophyllite-group minerals]. There is the [12]-coordinated C site, with $<C\text{–}O> = 3.570$ Å and in accord with the refined site-scattering of 3.32 $epfu$, we assign (0.06 Rb + 0.02 Cs) $apfu$ to the C site (Table 6).

Table 5. Selected distances (Å) and angles (°) for nafertisite.

Si(1)-O(3)		1.608(4)	Si(2)-O(4)	1.609(4)	Si(3)-O(9)	1.623(2)
Si(1)-O(2)a		1.612(4)	Si(2)-O(5)	1.620(4)	Si(3)-O(8)	1.636(4)
Si(1)-O(1)		1.633(4)	Si(2)-O(6)	1.628(4)	Si(3)-O(6)	1.639(4)
Si(1)-O(4)		1.641(4)	Si(2)-O(7)a	1.628(4)	Si(3)-O(7)b	1.641(4)
$<$Si(1)-O$>$		1.624	$<$Si(2)-O$>$	1.621	$<$Si(3)-O$>$	1.635
M(1)-X^O_A(2)		2.093(4)	M(2)-X^O_A(2)b	2.088(3)	M(3)-X^O_A(1)a	2.104(5)
M(1)-X^O_A(1)		2.092(3)	M(2)-O(5)3	2.097(3)	M(3)-X^O_D b	2.133(5)
M(1)-O(1)a		2.108(3)	M(2)-O(8)b	2.118(4)	M(3)-O(1) x2	2.171(4)
M(1)-O(8)		2.125(3)	M(2)-O(5)	2.122(3)	M(3)-O(8)b x2	2.181(4)
M(1)-O(5)		2.183(3)	M(2)-X^O_A(2)	2.138(4)	$<$M(3)-$\varphi>$	2.157
M(1)-X^O_D		2.205(3)	M(2)-O(1)	2.154(4)		
$<$M(1)-$\varphi>$		2.134	$<$M(2)-$\varphi>$	2.120	Si(1)-O(4)-Si(2)	144.4(3)
					Si(2)-O(6)-Si(3)	140.9(3)
D-X^O_D b		1.807(5)	B-O(3) x4	2.652(4)	Si(2)a-O(7)-Si(3)b	141.3(3)
D-O(2)c	x2	1.948(4)	B-O(2)a x4	2.655(4)	Si(3)-O(9)-Si(3)d	140.0(4)
D-O(3)	x2	1.952(4)	B-X^P_D f x2	2.6791(5)	$<$Si-O-Si$>$	141.7
D-X^P_D		2.143(1)	$<$B-$\varphi>$	2.659		
$<$D-$\varphi>$		1.958			C-O(6) x4	3.532(4)
					C-O(7)a x4	3.569(4)
A(1)-O(2)b	x2	2.826(9)	A(2)-W	2.21(1)	C-O(9) x4	3.609(5)
A(1)-O(3)	x2	2.829(9)	A(2)-X^P_D	2.309(5)	$<$C-O$>$	3.570
A(1)-X^P_D		3.05(1)	A(2)-O(2)b x2	2.464(4)		
A(1)-O(4)e	x2	3.512(4)	A(2)-O(3) x2	2.467(4)	Short distances	
A(1)-O(4)	x2	3.515(4)	$<$A(2)-$\varphi>$	2.397	A(1)-A(2)	0.74(1)
$<$A(1)-$\varphi>$		3.157			A(1)-W	1.47(2)

φ = O, F, OH, H_2O.
Symmetry operators: a: $-x, -y + \frac{1}{2}, -z + \frac{1}{2}$; b: $-x + 1, -y + \frac{1}{2}, -z + \frac{1}{2}$; c: $-x + 1, y + \frac{1}{2}, -z + \frac{1}{2}$; d: $x, -y, z$; e: $\times + 1, y, z$; f: $x\text{-}1, y, z$;

Table 6. Refined site-scattering and assigned site-populations for nafertisite.

Site*	Refined site-scattering (*epfu*)	Assigned site-population (*apfu*)	Calculated site-scattering (*epfu*)	$\langle X$–$\varphi\rangle_{obs.}$ (Å)	Ideal composition (*apfu*)
$T(1$–$4)$		11.81 Si + 0.19 Al		1.627	Si$_{12}$
$M(1)$	102.2(5)	9.11Fe^{2+} + 0.46 Mg + 0.22 Mn +		2.134	
$M(2)$	99.5(5)	0.10Al + 0.09 Na + 0.02 Ca		2.120	
$M(3)$	51.0(3)			2.157	
ΣM	252.7		250.57		Fe$^{2+}{}_{10}$
D	44.6(3)	1.90 Ti + 0.05 Nb + 0.03 Mg + 0.02 Zr	45.01	1.958	Ti$_2$
$^{[9]}A(1)$	11.59	1.39 □ + 0.61 K	11.59	3.157	
$A(2)$	15.29	1.39 Na + 0.61 □	15.29	2.397	
$\Sigma A**$	26.88	1.39 Na + 0.61 K	26.88		Na$_2$
$^{[10]}B$	11.0	1.0 Na	11.0	2.659	Na
$^{[12]}C$	3.32	0.92 □ + 0.06 Rb + 0.02 Cs	3.32	3.570	□
$X_A^O(1)$		2 (OH)			(OH)$_2$
$X_A^O(2)$		4 (OH)			(OH)$_4$
X_D^P		0.86 F + 0.14 O			F
W		1.39 (H$_2$O) + 0.61 □			(H$_2$O)$_2$***

* coordination number is given for non-[6]-coordinated sites;
** A(1)–A(2) = 0.74 Å (see Table 5);
*** the Na atom at the $A(2)$ site is coordinated by four O atoms, F atom [X_D^P] and an H$_2$O group at the W site. The content of Na at the A [$=A(1)+A(2)$] site strongly correlates with the content of H$_2$O at the W site. The ideal composition of the A site is Na$_2$ and we must write the ideal composition of the W site as (H$_2$O)$_2$ *pfu*.

Table 7. Bond-valence values for nafertisite.*

Atom	T(1)	T(2)	T(3)	M(1)	M(2)	M(3)	D	A(1)	A(2)	B	H(1)	H(2)	Σ
O(1)	0.97			0.38	0.33	0.32$^{\times2\downarrow}$							2.04
$^{[5]}$O(2)	1.03						0.67$^{\times2\downarrow}$	0.04$^{\times2\downarrow}$	0.12$^{\times2\downarrow}$	0.12$^{\times4\downarrow}$		0.02	2.00
O(3)	1.04						0.67$^{\times2\downarrow}$	0.04$^{\times2\downarrow}$	0.12$^{\times2\downarrow}$	0.12$^{\times4\downarrow}$			1.99
O(4)	0.95	1.04						0.01$^{\times2\downarrow}$				0.02	2.03
								0.01$^{\times2\downarrow}$					
O(5)		1.01		0.31	0.39								2.07
					0.36								
O(6)		0.98	0.96										1.94
O(7)		0.98	0.95								0.01$^{\times2\downarrow}$		1.94
O(8)			0.96	0.36	0.37	0.31$^{\times2\downarrow}$							2.00
O(9)			1.00$^{\times2\rightarrow}$										2.00
X_D^O				0.29$^{\times2\rightarrow}$		0.35	1.00						1.93
$^{[3]}X_A^O(1)$				0.39$^{\times2\rightarrow}$		0.38					0.98		2.14
$^{[3]}X_A^O(2)$				0.39	0.40							0.96	2.10
					0.35								
$^{[6]}X_D^P$							0.28$^{\times2\rightarrow}$	0.03$^{\times2\rightarrow}$	0.12$^{\times2\rightarrow}$	0.09$^{\times2\downarrow\rightarrow}$			1.04
$^{[1]}W$									0.19				0.19
Total	3.99	4.01	3.87	2.12	2.20	1.99	3.96	0.23	0.79	1.14	1.00	1.00	
Aggreg. charge	3.98	3.98	3.98	2.00	2.00	2.00	4.00	0.31	0.70	1.00	1.00	1.00	

*Bond-valence parameters are from Brown (1981) and Brown & Altermatt (1985); coordination numbers are shown for non-[4]-coordinated anions and H$_2$O groups.

After assignment of cations to the H sheet and **I** block, we are left with (9.11 Fe^{2+} + 0.46 Mg + 0.22 Mn + 0.10 Al + 0.09 Na + 0.02 Ca)$_{\Sigma10}$ *apfu*, with an aggregate scattering of 250.57 *epfu* to assign to the three M sites in the O sheet. The total refined scattering at these sites is 252.7 *epfu* (Table 6) and, thus, supports this assignment.

7.3. Description of the structure

7.3.1. Site nomenclature

As stated above, the cation sites are divided into three groups: M sites of the O sheet, D and T sites of the H sheet, and interstitial sites in the **I** block. By analogy with

the TS-block minerals (Sokolova, 2006), we label the X anions (which do not bond to T cations) as follows: X^O anions occur in the O sheet; X_D^O = anion at the common vertex of four polyhedra, three M and D; X_A^O = anion at the common vertex of four polyhedra, 3 M and A (or C), where A^P–$X_A^O \leq 3$ Å or at the common vertex of three M octahedra where A^P–$X_A^O > 3$ Å, and hence the X_A^O anion does not coordinate the A (or C) atom; X_D^P = apical anion of D cation at the periphery of the HOH layer.

7.3.2. Cation sites

Here we will describe the cation sites of the O sheet, H sheets and interstitial A, B and C sites. In the O sheet, there are three [6]-coordinated Fe^{2+}-dominant M sites with 100%-occupancy (Table 6, Fig. 3a). The $M(1)$ and $M(2)$ sites are coordinated by four O atoms and two X_A^O anions [$X_A^O(1) = X_A^O(2)$ = OH, see section *Anion considerations* below] with <$M(1)$–φ> and <$M(2)$–φ> distances of 2.134 and 2.120 Å, respectively (φ = unspecified anion) (Tables 5 and 6). The $M(3)$ site is coordinated by five O atoms and the $X_A^O(1)$ anion, with <$M(3)$–φ> distance of 2.157 Å (Tables 5 and 6). For the O sheet, the total of the 10 M cations is ($Fe^{2+}_{9.11}Mg_{0.46}Mn_{0.22}Al_{0.10}$ $Na_{0.09}Ca_{0.02})_{\sum10}$, with an ideal composition Fe^{2+}_{10} *apfu*.

In the H sheet, there are three tetrahedrally coordinated T sites occupied mainly by Si and minor Al, with a <T–O> distance of 1.627 Å (Tables 5 and 6). The [6]-coordinated D site is occupied by (1.90 Ti + 0.05 Nb + 0.02 Zr + 0.03 Mg) *apfu* (Table 6) and is coordinated by five O atoms and a F atom at the X_D^P site (Fig. 3a), with <M^H–φ> = 1.958 Å, a short D–X_D^O distance of 1.807 and a long M^H–X_D^P distance of 2.143 Å (Table 5), in accord with the structure topology of astrophyllite-group minerals (Sokolova, 2012). For the H sheets, the total of 2D cations is ideally Ti_2 *apfu*.

In the I block of nafertisite, there are three interstitial cation sites, A, B and C. The A site is split into two sites, the [9]-coordinated $A(1)$ site and the [6]-coordinated $A(2)$ site that are only 0.74 Å apart (Fig. 3b, Table 5). A similar separation of the split A site occurs in several astrophyllite-group minerals: niobokupletskite, $K_2NaMn_7(Nb,Ti)_2$ $(Si_4O_{12})_2O_2$ $(OH)_4(O,OH)$ (Piilonen *et al.*, 2000); nalivki-nite $Li_2NaFe^{2+}_7Ti_2(Si_4O_{12})_2O_2(OH)_4F$ (Uvarova *et al.*, 2008), kupletskite-Cs, $Cs_2NaMn_7Ti_2(Si_4O_{12})_2O_2(OH)_4F$ (Cámara *et al.*, 2010), *etc*. The $A(1)$ site is occupied by K at 30 % and it is coordinated by eight O atoms and a F atom at the X_D^P site, with <$A(1)$–φ> = 3.157 Å (Tables 5 and 6). The $A(2)$ site is occupied by Na at 70 % and it is coordinated by four O atoms, a F atom at the X_D^P site and an H_2O group at the W site, with <$A(2)$–φ> = 3.157 Å (Tables 5 and 6). Cations at the A site sum to ($Na_{1.39}K_{0.61})_{\Sigma2}$ *apfu*, Na is the dominant cation species, and we write simplified and ideal compositions of the A site as (Na,K) and Na_2 *pfu*, respectively. Figure 3c shows a possible short-range-order (SRO) arrangement of K and Na atoms where they fully occupy the $A(1)$ and $A(2)$ sites, respectively. The B site is occupied by Na *apfu*
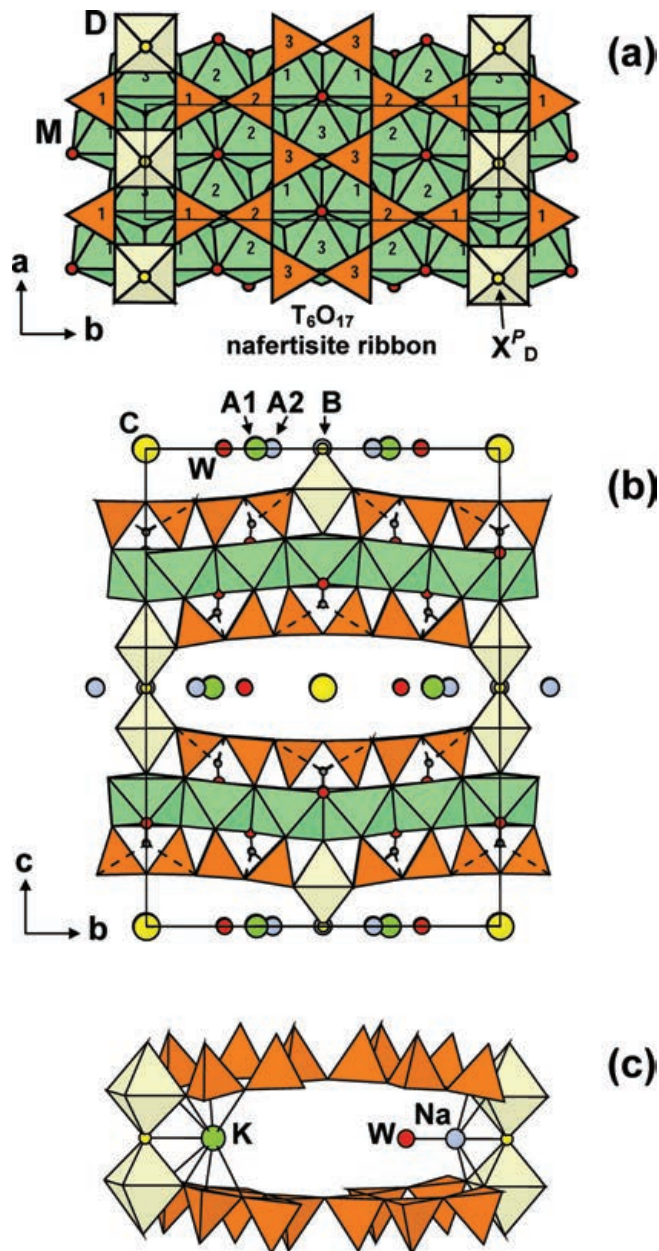
Fig. 3. The crystal structure of nafertisite: (a) linkage of H and O sheets in the HOH layer; (b) general view of the structure: self-linkage of adjacent HOH layers via D-X_D^P-D bridges; (c) a possible short-range-order (SRO) arrangement of K and Na atoms at the $A(1)$ and $A(2)$ sites, respectively. Si tetrahedra are orange, Ti-dominant D and Fe^{2+}-dominant M octahedra are yellow and green, Na [$A(2)$, B sites], K [$A(1)$ site] and (Rb,Cs) [C site] atoms are shown as medium blue and large green and yellow spheres, X_D^P (=F) anions and OH groups are shown as small yellow and red spheres; an H_2O group [W site] is shown as a medium red sphere, H atoms are shown as small grey spheres, hydrogen bonds are shown as dashed black lines; the unit cell is shown with thin black lines.

(Table 6) and it is [10]-coordinated by eight O atoms and two F atoms at the X_D^P sites, with <B–φ> = 2.659 Å (Table 5). The [12]-coordinated C site is occupied by (Rb + Cs) at 8

% (Table 6), $<C–O> = 3.570$ Å (Table 5). The ideal composition of the *C* site is $\square$ *pfu*.

We write the cation part of the ideal structural formula as the sum of cations (i) at the interstitial *A, B* and *C* sites + (ii) of the O sheet + (iii) of two H sheets: (i) Na$_3\square$ + (ii) Fe$^{2+}_{10}$ + (iii) Ti$_2$ = Na$_3$Fe$^{2+}_{10}$Ti$_2$ with a total charge of 31^+.

7.3.3. Anion considerations

There are seven anion sites, O(1–9), occupied by O atoms which form the tetrahedral coordination of the T atoms and have bond-valence sums of 1.94–2.07 *vu* (valence units) (Tables 5 and 7). An anion common to the D octahedron and three octahedra of the O sheet occurs at the X^O_D site (Table 7, Fig. 3a), it receives bond valences of 1.93 *vu* (Table 7) and hence is an O atom. The anions at the $X^O_A(1,2)$ sites are O atoms of OH groups (Tables 6 and 7). Each OH group is bonded to three M cations of the O sheet (Fig. 3a). The H(1) and H(2) atoms are involved in a weak hydrogen bonding with O atoms that belong to the H sheets (Table 8, Fig. 3b). The two $X^O_A(1,2)$ sites give (OH)$_6$ *pfu* (Table 6). The X^P_D anion occurs at the periphery of the HOH layer and is a bridge anion for two D cations (Tables 6 and 7); it receives bond valence of (0.28×2) *vu* from two D cations, 0.30 *vu* from two A(1,2) cations and 0.18 *vu* from two B cations (Table 9), and has the following composition F$_{0.86}$O$_{0.14}$ *pfu* (Table 6). Occurrence of F at the X^P_D site is quite common for most astrophyllite-group minerals (Sokolova, 2012).

There is an H$_2$O group which occurs at the *W* site, with the composition $[(H_2O)_{1.39}\square_{0.61}]$ *pfu* (Tables 6 and 7). This H$_2$O group is bonded to a Na atom at the *A*(2) site (Fig. 3c). There are two ways to write the ideal composition of the *W* site. Arithmetic tells us to round (H$_2$O)$_{1.39}$ to (H$_2$O)$_1$ *pfu*. However, in accord with the IMA rules, we write the ideal composition of the *A* site as Na$_2$ (see above; *cf.* Na$_{1.39}$K$_{0.61}$ *apfu*, Table 6). Na at the *A* site requires H$_2$O at the *W* site to be properly coordinated (Table 5), but the *W* site cannot be occupied when K is at the *A* site. Hence we write the ideal composition of the *W* site as (H$_2$O)$_2$ *pfu* (Table 6).

We write the anion part of the ideal formula as the sum of the anions at the following sites: O$_{34}$ (O atoms of Si$_{12}$ tetrahedra) + O$_2$ [X^O_D] + (OH)$_6$ [$X^O_A(1,2)$] + F [X^P_D] + (H$_2$O)$_2$ [*W*]. We consider the nafertisite T$_6$O$_{17}$ ribbon as a complex oxyanion and write the anion part of the ideal

structural formula as $(Si_6O_{17})_2O_2(OH)_6F(H_2O)_2$, with a total charge of 31^-.

We write the ideal formula of nafertisite as the sum of the cation and anion parts:

$$Na_3Fe^{2+}_{10}Ti_2(Si_6O_{17})_2O_2(OH)_6F(H_2O)_2, Z = 2.$$
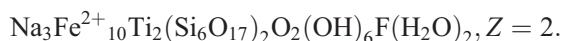
7.3.4. Structure topology

The HOH layer is the main structural unit in the crystal structure of nafertisite. The central O sheet is composed of Fe^{2+}-dominant M octahedra and has ideal composition Fe$^{2+}_{10}$ *apfu*. The H sheet is built of nafertisite T$_6$O$_{17}$ ribbons and Ti-dominant D octahedra (Fig. 3a). Two H sheets connect to the O sheet via common vertices of M octahedra of the O sheet and D and T polyhedra of the H sheets (Fig. 3a and b). Adjacent HOH layers link via X^P_D anions at common vertices of D octahedra, forming D-X^P_D-D bridges as in astrophyllite (Fig. 3b). The structure topology of the HOH layer is in accord with Ferraris *et al.* (1996).

In the O sheet, each M octahedron shares at least one edge with an Si$_2$O$_7$ group of the H sheet and the sizes of the M octahedra follow the pattern M(3) > M(1) > M(2). Sokolova (2012) showed that in the astrophyllite-group minerals, the sizes of M octahedra in the O sheet are different due to the different linkage of M octahedra and polyhedra of the H sheet. She showed that the smallest octahedron shares two edges with two Si$_2$O$_7$ groups of the astrophyllite ribbon, the larger octahedra share an edge with an Si$_2$O$_7$ group and a vertex with a Ti octahedron. This rule applies to the O sheet in nafertisite: the smallest M(2) octahedron [$<M(2)–\varphi> = 2.120$ Å] shares two edges with two Si$_2$O$_7$ groups of the nafertisite ribbon (Fig. 3a). Of two larger octahedra, the M(3) octahedron [$<M(3)–\varphi> = 2.157$ Å] is larger than the M(1) octahedron [$<M(1)–\varphi> = 2.134$ Å] due to different orientation of the attached Si$_2$O$_7$ groups (for details, see Sokolova, 2012).

In the structure, HOH layers alternate with **I** blocks along **c**. In the **I** block of nafertisite, the following cations occur: [6]Na, [9]K and minor [12]Rb (+Cs) (Fig. 3b). There is short-range order of K and Na at the *A* site and H$_2$O groups at the *W* site (Fig. 3c). The chemical composition of the **I** block of the formula A$_2$BCW is (Na$_{1.39}$K$_{0.61}$)Na($\square_{0.92}$Rb$_{0.06}$Cs$_{0.02}$)(H$_2$O$_{1.39}\square_{0.61}$) *pfu*, ideally Na$_3$(H$_2$O)$_2$ *pfu* (see discussion

---

Table 8. Hydrogen bonding in nafertisite.

D–H…A	D–H (Å)	H…A (Å)	D–A (Å)	$<$ DHA (°)
$X^O_A(1)(OH)$–H(1)…O(7)a	0.98(1)	2.93(3)	3.568(6)	123(2)
$X^O_A(1)(OH)$–H(1)…O(7)b	0.98(1)	2.93(3)	3.568(6)	123(2)
$X^O_A(2)(OH)$–H(2)…O(4)a	0.98(1)	2.68(5)	3.436(5)	134(5)
$X^O_A(2)(OH)$–H(2)…O(2)	0.99(1)	2.70(5)	3.448(6)	134(5)

a: -*x*, -*y* + ½, -*z* + ½; b: -*x*, *y*-½, -*z* + ½.

above). Na, K, Rb and Cs are common interstitial cations in the astrophyllite-group minerals and occur at the *A* and *B* sites (Cámara *et al.*, 2010). However, the *C* site is absent in the astrophyllite-group minerals. Occurrence of the *C* site is possible as there is a larger interstitial space in the nafertisite structure due to the triple nafertisite ribbons in the H sheet if compared to a smaller interstitial space associated with the double astrophyllite ribbons in the astrophyllite-group minerals.

8. Summary

(1) The general topology of the HOH layer in nafertisite is in accord with Ferraris *et al.* (1996). The H sheet is composed of the nafertisite T_6O_{17} ribbons and Ti-dominant D octahedra. The O sheet is composed of M(1–3) octahedra.

(2) In accord with the Mössbauer spectroscopy results, the O sheet is composed of Fe^{2+}-dominant M(1–3) octahedra, the $M(1–3)$ sites are 100 % occupied and the ideal composition of the O sheet is Fe^{2+}_{10} *apfu*.

(3) The empirical composition of the nafertisite Ti_6O_{17} ribbon is $(Si_{11.81}Al_{0.19})O_{34}$ *apfu*, ideally $(Si_6O_{17})_2$ *pfu*.

(4) In the crystal structure of nafertisite, HOH layers alternate with **I** blocks along **c**. The ideal composition of the **I** block of the formula A_2BCW is $Na_3\square(H_2O)_2$ *pfu*.

(5) The empirical formula of nafertisite calculated on the basis of $(O + F + OH + H_2O) = 44.39$ *pfu* is as follows $(Na_{1.39}K_{0.61})_{\Sigma2}Na_1(\square_{0.92}Rb_{0.06}Cs_{0.02})_{\Sigma1}(Fe^{2+}_{9.11}Mg_{0.46}Mn_{0.22}Al_{0.10}Na_{0.09}Ca_{0.02})_{\Sigma10}(Ti_{1.90}Nb_{0.05}Mg_{0.03}Zr_{0.02})_{\Sigma2}[(Si_{11.81} Al_{0.19})_{\Sigma12}O_{34}]O_2(OH)_6(F_{0.86}O_{0.14})_{\Sigma1}(H_2O)_{1.39}$; and the ideal chemical formula of nafertisite is $Na_3Fe^{2+}_{10}Ti_2(Si_6O_{17})_2O_2(OH)_6F(H_2O)_2$, Z = 2.

References

Abdu, Y.A., Scorzelli, R.B., Varela, M.E., Kurat, G., Souza Azevedo, I., Stewart, S.J., Hawthorne, F.C. (2009): Druse clinopyroxene in D'Orbigny angritic meteorite studied by single-crystal X-ray diffraction, electron microprobe analysis and Mössbauer spectroscopy. *Met. Planet. Sci.*, **44**, 581–587.

Belov, N.V. (1976): Essays on structural mineralogy. Nedra, Moscow. (in Russian)

Brown, I.D. (1981): The bond valence method: an empirical approach to chemical structure and bonding. *in* ''Structure and Bonding in Crystals II'', M. O'Keeffe & A. Navrotsky, eds. Academic Press, New York, NY, 1–30.

Brown, I.D. & Altermatt, D. (1985): Bond-valence parameters obtained from a systematic analysis of the inorganic crystal structure database. *Acta Crystallogr.*, **B41**, 244–247.

Cámara, F., Sokolova, E., Abdu, Y., Hawthorne, F.C. (2010): The crystal structures of niobophyllite, kupletskite-(Cs) and Sn-rich astrophyllite; revisions to the crystal chemistry of the astrophyllite-group minerals. *Can. Mineral.*, **48**, 1–16.

Cámara, F., Sokolova, E., Hawthorne, F.C., Rowe, R., Grice, J.D., Tait, K.T. (2013): Veblenite, $K_2\square_2Na(Fe^{2+}_5Fe^{3+}_4Mn^{2+}_7\square)Nb_3Ti(Si_2O_7)_2(Si_8O_{22})_2O_6(OH)_{10}(H_2O)_3$, a new mineral from Seal Lake, Newfoundland and Labrador: mineral description, crystal structure, and a new veblenite (Si_8O_{22}) ribbon. *Mineral. Mag.*, **77**, 2955–2974.

Ferraris, G., Ivaldi, G., Khomyakov, A.P., Soboleva, S.V., Belluso, E., Pavese, A. (1996): Nafertisite, a layer titanosilicate member of a polysomatic series including mica. *Eur. J. Mineral.*, **8**, 241–249.

Khomyakov, A.P., Ferraris, G., Ivaldi, G., Nechelyustov, G.N., Soboleva, S.V. (1995): Nafertisite, $Na_3(Fe^{2+},Fe^{3+})_6[Ti_2Si_{12}O_{34}](O,OH)_7?2H_2O$, a new mineral with a new type of banded silicate radical. *Zap. Vser. Mineral. Obshch.*, **124**, 101–107. (in Russian)

Khomyakov, A.P., Cámara, F., Sokolova, E., Hawthorne, F.C., Abdu, Y. (2011): Sveinbergeite, $Ca(Fe^{2+}_6Fe^{3+})Ti_2(Si_4O_{12})_2O_2(OH)_5(H_2O)_4$, a new astrophyllite-group mineral species from the Larvik plutonic complex, Oslo region, Norway: description and crystal structure. *Mineral. Mag.*, **75**, 2687–2702.

Layne, G.D., Rucklidge, J.C., Brooks, C.K. (1982): Astrophyllite from Kangerdlugssuaq, East Greenland. *Mineral. Mag.*, **45**, 149–156.

Liebau, F. (1985): Structural chemistry of silicates. Springer-Verlag, Berlin.

Petersen, O.V., Johnsen, O., Christiansen, C.C., Robinson, G.W., Niedermayr, G. (1999): Nafertisite – $Na_3Fe_{10}Ti_2Si_{12}(O,OH,F)_{43}$ –from the Nanna pegmatite, Narsaarsuup Qaava, South Greenland. *N. Jb. Mineral. Mh.*, **1999**, 303–310.

Piilonen, P.C., Lalonde, A.E., McDonald, A.M., Gault, R.A. (2000): Niobokupletskite, a new astrophyllite-group mineral from Mont Saint-Hilaire, Quebec, Canada: Description and crystal structure. *Can. Mineral.*, **38**, 627–639.

Pouchou, J.L. & Pichoir, F. (1985): PAP' φ(ρZ) procedure for improved quantitative microanalysis. *in* ''Microbeam analysis'', J.T. Armstrong, ed. San Francisco Press, San Francisco, 104–106.

Shannon, R.D. (1976): Revised effective ionic radii and systematic studies of interatomic distances in halides and chalcogenides. *Acta Crystallogr.*, **A32**, 751–767.

Sheldrick, G.M. (2004): CELL_NOW. University of Göttingen, Germany.

— (2008a): TWINABS. University of Göttingen, Germany.

— (2008b): A short history of SHELX. *Acta Crystallogr.*, **A64**, 112–122.

Sokolova, E. (2006): From structure topology to chemical composition. I. Structural hierarchy and stereochemistry in titanium disilicate minerals. *Can. Mineral.*, **44**, 1273–1330.

— (2012): Further developments in the structure topology of the astrophyllite-group minerals. *Mineral. Mag.*, **76**, 863–882.

Sokolova, E., Hawthorne, F.C., Abdu, Y.A. (2013): From structure topology to chemical composition. XV. Titanium silicates: revision of the crystal structure and chemical formula of schüllerite, $Na_2Ba_2Mg_2Ti_2(Si_2O_7)_2O_2F_2$, from the Eifel volcanic region, Germany. *Can. Mineral.*, **51**, 715–725.

Uvarova, Y.A., Sokolova, E., Hawthorne, F.C., Agakhanov, A.A., Pautov, L.A. (2008): The crystal structure of nalivkinite, a new lithium member of the astrophyllite group. *Can. Mineral.*, **46**, 651–659.

Wilson, A.J.C. ed (1992): International tables for crystallography. volume C: mathematical, physical and chemical tables. Kluwer Academic Publishers, Dordrecht, The Netherlands.